Available online at www.sciencedirect.com
SCIENCE DIRECT®
ELSEVIER
C. R. Mecanique 334 (2006) 259–265
COMPTES RENDUS
MECANIQUE
http://france.elsevier.com/direct/CRAS2B/

Active control of the aeroacoustics of cavity flows from the downstream edge

Ludovic Chatellier [a,*], Janick Laumonier [a], Yves Gervais [b]

[a] *Laboratoire d'études aérodynamiques, UMR CNRS 6609, bâtiment K, 40, avenue du Recteur Pineau, 86022 Poitiers cedex, France*
[b] *Laboratoire d'études aérodynamiques, UMR CNRS 6609, bâtiment H, 40, avenue du Recteur Pineau, 86022 Poitiers, France*

Received 21 May 2004; accepted after revision13 January 2006

Presented by Sébastien Candel

Abstract

Active control of the aeroacoustics of flow-induced oscillations in a rectangular cavity using a vibrating plate inserted at the downstream edge is demonstrated. Pressure and phase-locked Particle Image Velocimetry measurements show that the oscillations of the mixing layer can be controlled in order to attenuate or amplify the radiated sound. Results obtained from a previously developed analytical model are used to characterize the effects of the control. ***To cite this article: L. Chatellier et al., C. R. Mecanique 334 (2006).***

Résumé

On présente le contrôle actif des instabilités aéroacoustiques générées en cavité sous écoulement affleurant effectué à l'aide de la mise en vibration du bord aval de la cavité. Mesures de pression et vélocimétrie par images de particules synchronisée montrent qu'il est possible de moduler l'amplitude des oscillations de la couche de mélange afin d'atténuer ou d'amplifier le bruit rayonné par l'écoulement. Les résultats fournis par un modèle analytique développé au préalable permettent de caractériser les effets du contrôle. ***Pour citer cet article : L. Chatellier et al., C. R. Mecanique 334 (2006).***

Keywords: Fluid mechanics; Acoustics; Experimental; Instability; Control; PIV

Mots-clés : Mécanique des fluides ; Acoustique ; Expérimental ; Instabilité ; Contrôle ; PIV

1. Introduction

As it has been shown that passive control of the self sustained oscillations generated in cavity flows could only be demonstrated for a limited range of conditions [1–4], a number of authors have focused on the possibility of applying

* Corresponding author. Present address: Laboratoire d'étude des phénomènes de transfert appliqués au bâtiment, pôle sciences et technologie, avenue Michel-Crépeau, 17024 La Rochelle cedex 1, France.

E-mail addresses: ludovic.chatellier@univ-lr.fr (L. Chatellier), janick.laumonier@lea.univ-poitiers.fr (J. Laumonier), yves.gervais@lea.univ-poitiers.fr (Y. Gervais).

1631-0721/$ – see front matter
doi:10.1016/j.crme.2006.03.003

pseudo-active or active control using loudspeakers [5–7], fluidic actuators [8,9] or mechanical devices [10,11]. It has also been established that self-sustained oscillations of cavity flows are a result of the receptivity of the upstream region to the disturbance produced in the downstream region. Consequently, a successful control applied to the slightly perturbed upstream region would minimize the energy cost. In comparison, a successful control of the disturbance created in the downstream region would inhibit the feedback source and cancel its effects on the upstream region. It has been shown that active control from the upstream edge can be achieved [9,11,12] and simulated numerically [12]. Simulations of Kestens [13,14] indicate that a combination of upstream and downstream actuators can improve the efficiency of the control. Thus, the present study proposes a novel method of control using a vibrating plate located at the downstream edge of the cavity. It is argued that such a strategy would benefit from the mixing layer receptivity to the presence of moving boundaries, as suggested by Rockwell and Naudasher [15].

2. Experimental apparatus

The experiments were carried out in a parallelepipedic cavity of adjustable dimensions installed in an Eiffel-type circular wind-tunnel. The setup and experimental conditions are discussed in detail in Chatellier et al. [16]. The actuator depicted in Fig. 1 consists in a 300 mm × 30 mm aluminium plate located at the downstream edge of the cavity and placed half-way along the wingspan. The plate is attached to an electromagnetic vibrator which generates a piston-like motion along the main flow direction. An accelerometer attached to the moving plate is used to record the local vibration level during control. The control circuit is based on a frequency-tracking board initially used to allow phase-locked PIV measurements. The first stage consists in a narrow band-pass filter used to isolate the frequency of a mode of interest. The second stage transforms the filtered signal into a periodic square wave using a trigger. A low-pass filter finally extracts the fundamental frequency of the square wave as a sine wave of fixed amplitude. Control parameters consist in the absolute amplitude and relative phase of the command signal which are manually adjusted in the two last stages of the circuit.

As explained in [17], the actuator has been designed so that its dynamic response allows a maximum of efficiency in the range of frequencies corresponding to the oscillation modes. Preliminary tests have been carried out for a matching cavity width ($W = 0.3$ m) and have led to satisfactory results. Subsequent tests at full width ($W = 0.78$ m) using the same actuator resulted in an improved control of the noise level, even though the actuator occupies less than 40% of the cavity width. Results presented in what follows pertain to the latter configuration, for which the length, depth and width of the cavity are respectively $L = 0.15$ m, $D = 0.15$ m and $W = 0.78$ m.

The acoustic signature of this cavity geometry is presented in Figs. 2(a) and (b). The first high level band appearing in Fig. 2(a) corresponds to the noise generated by the wind-tunnel's variable-speed fan. Up to five modes of oscillations can be identified, which exhibit power densities at quasi-constant Strouhal numbers, as shown in Fig. 2(b). Previous phase-locked PIV measurements [16] have confirmed that these oscillation modes are essentially driven by convective waves, also described as *operating stages* in the theoretical analyses of Howe [18–20]. These operating stages locally interact with three resonance modes occurring between the cavity floor and the upper part of the test section, resulting

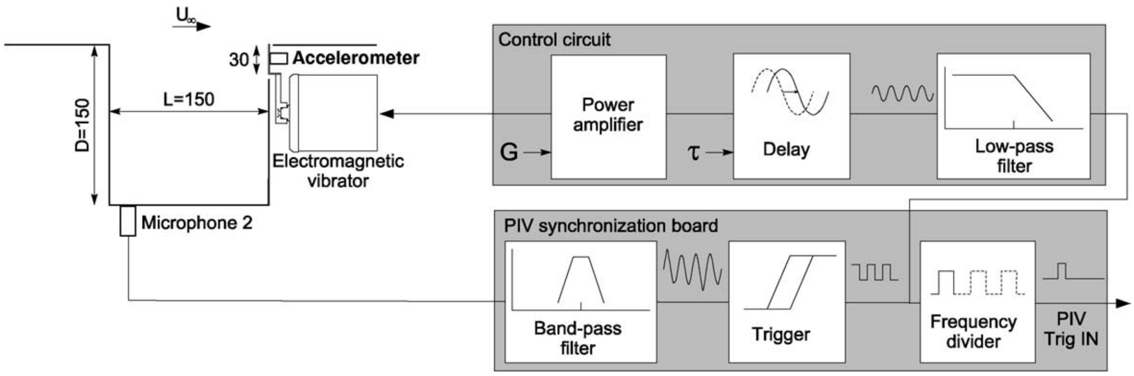

Fig. 1. Overview of the active control setup and command circuit.

Fig. 1. Aperçu du dispositif de contrôle actif et du circuit de commande.

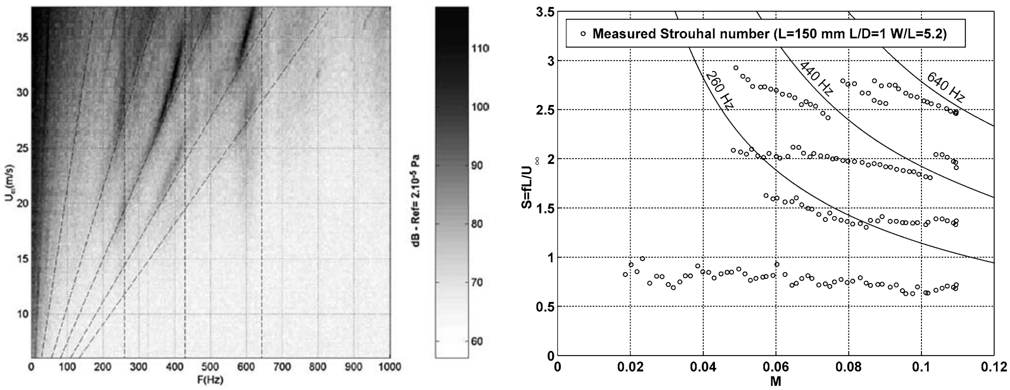

(a) (b)

Fig. 2. (a) Pressure spectra measured by Microphone 2; (b) Corresponding Strouhal number versus Mach number distribution (b); $L = 150$ mm, $W/L = 5.2$, $L/D = 1$.

Fig. 2. Spectres de pression measurés par le Microphone 2 (a) et distribution des nombres de Strouhal correspondants en fonction du nombre de Mach (b) ; $L = 150$ mm, $W/L = 5{,}2$, $L/D = 1$.

Table 1
Flow regimes and oscillation modes chosen for active-control

Tableau 1
Regimes de vitesse et modes d'oscillations retenus pour l'application du contrôle actif

$U_\infty (\mathrm{m\,s^{-1}})$	2nd mode	3rd mode
29.8	255 Hz, no coupling	380/387 Hz, weak coupling
30.1	257 Hz, weak coupling	387 Hz, strong coupling
31	257 Hz, weak coupling	391 Hz, strong coupling

in aeroacoustic couplings which appear at 260, 440 and 640 Hz. Further details concerning the nature of the unforced flow can be found in Chatellier et al. [16].

Control was applied at three flow velocities chosen between 29 and 31 $\mathrm{m\,s^{-1}}$, for which the second and third mode of oscillation respectively lead to weak and strong aeroacoustic couplings with the resonant frequencies of the apparatus at 260 and 440 Hz. The flow regimes are listed in Table 1. Over the narrow velocity range considered, the second mode triggers a weak aeroacoustic coupling around 255 Hz which tends to vanish for $U_\infty > 31\ \mathrm{m\,s^{-1}}$, whereas the third mode triggers a strong aeroacoustic coupling at 387 Hz which reaches a maximum level around $U_\infty = 31\ \mathrm{m\,s^{-1}}$ (Fig. 2(a)). At these regimes, the signal-to-noise ratio of the second mode is 8 to 12 dB and the signal-to-noise ratio of the third mode is 18 to 25 dB, offering an efficient tracking of the frequencies of interest and allowing application of the control. However, the phase-locked PIV measurements suffer from a relatively large jitter for modes at low signal-to-noise ratios. In consequence, the PIV results were considered valid only for the third mode of oscillations, for which the RMS jitter is around 89 µs at $U_\infty = 29.8\ \mathrm{m\,s^{-1}}$ and around 41 µs at $U_\infty = 31\ \mathrm{m\,s^{-1}}$, which respectively correspond to 3.4 and 1.6% of the period of interest.

3. Control results

3.1. Mode amplification

The ability of the active control system to generate a fluid-elastic mode was first investigated. This type of oscillating mode where the fluid motion couples with a moving or vibrating surface is examined by Rockwell and Naudascher [15] and is the underlying concept of the control method proposed in this note. It is also known that passive elements can be used to generate fluid-elastic modes, leading to a strategy of active control which consists in forcing the phase and amplitude of the moving element in order to induce such a mode of oscillation.

Figs. 3(a)–(c) show how mode 2 can be enhanced by an artificial fluid-elastic mode which will generate an intense aeroacoustic coupling with the acoustic resonance at 260 Hz. For this mode, the natural cycle of oscillation is not sufficiently powerful to lead to a strong, definite fluid-resonant mode as it happens for mode 3. Then, and though a weak natural aeroacoustic coupling is generated around $U_\infty = 30.1\ \mathrm{m\,s^{-1}}$ which locally enhances the efficiency of the control, the energy provided by the vibrating surface has a dramatic effect on the natural mode of oscillations. This results in a gain up to 17 dB for the pressure fluctuations, making mode 2 comparable to the naturally coupled mode 3.

The control applied to the third mode of oscillations leads to similar results, as shown in Figs. 3(c)–(e). Here, the natural oscillations at $U_\infty = 29.8\ \mathrm{m\,s^{-1}}$ tend to generate a weak fluid-resonant coupling which is not yet stabilized,

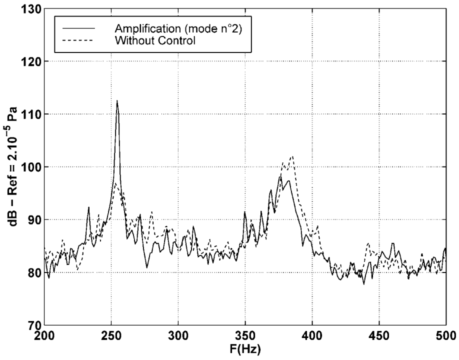

(a) Mode n° 2, $U_\infty = 29.8\ \mathrm{m.s^{-1}}$

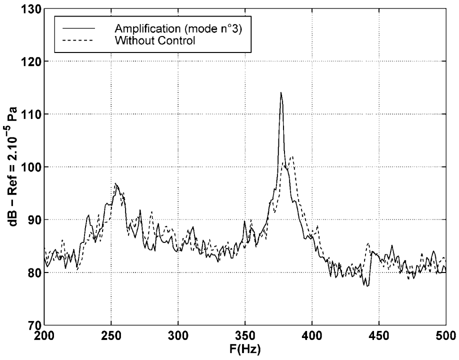

(d) Mode n° 3, $U_\infty = 29.8\ \mathrm{m.s^{-1}}$

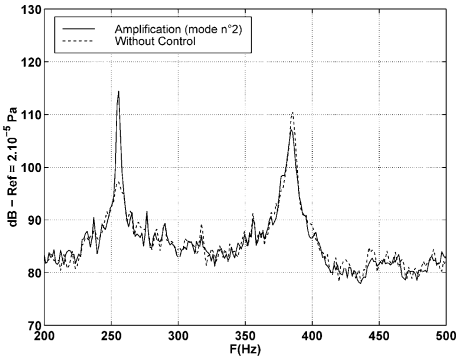

(b) Mode n° 2, $U_\infty = 30.1\ \mathrm{m.s^{-1}}$

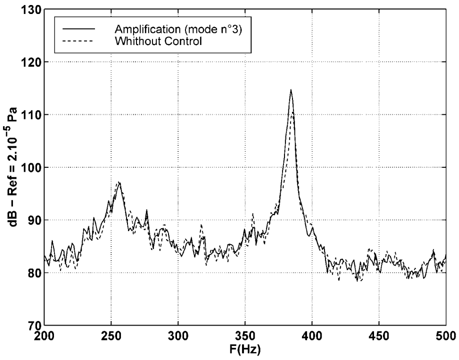

(e) Mode n° 3, $U_\infty = 30.1\ \mathrm{m.s^{-1}}$

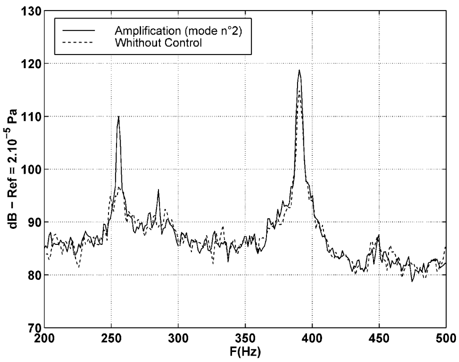

(c) Mode n° 2, $U_\infty = 31\ \mathrm{m.s^{-1}}$

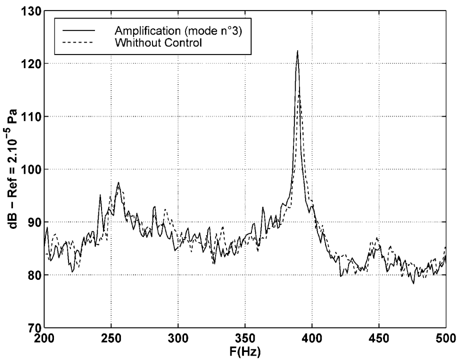

(f) Mode n° 3, $U_\infty = 31\ \mathrm{m.s^{-1}}$

Fig. 3. Amplification of the oscillation modes with and without aeroacoustic coupling. Mode 2: (a) no coupling, (b) weak coupling, (c) decaying weak coupling. Mode 3: (d) weak coupling, (e) strong coupling, (f) coupling at maximum intensity.

Fig. 3. Amplification des modes d'oscillation avec et sans présence de couplage aéroacoustique. Mode 2 : (a) pas de couplage ; (b) couplage faible ; (c) couplage faible dégradé. Mode 3 : (d) couplage faible ; (e) couplage fort ; (f) couplage au maximum d'intensité.

oscillating between 380 and 387 Hz. The reinforcement provided by the fluid-elastic coupling results in a fluid-resonant mode appearing around 380 Hz, a slightly lower frequency than the one measured under natural operating conditions. Further analysis of the acoustics of the apparatus indicate that secondary resonant modes are distributed between the three main acoustic modes, which may explain the double peaks in Figs. 3(a) and (b) and the shift towards a coupling at a lower frequency.

3.2. Mode attenuation

The second part of the experiments focuses on the ability of the apparatus to counteract the natural oscillation modes by locally forcing an out-of-phase boundary condition at the downstream edge. Here, the success of the strategy depends on the possibility of controlling the fluid motion where the oscillations are the largest, in order to prevent feedback to the leading edge.

Because the control affects the boundary conditions in order to phase the natural mode out, the characteristics of the setup are dynamically altered and marginal modes can be reinforced erratically. As a result, Figs. 4(a) and (b) show that weakly coupled mode 2 can be attenuated of 3 to 5 dB, while the frequency displacement cannot always be efficiently tracked, most probably because of the unsteadiness of the marginal modes. This appears clearly in Fig. 4(a) where the control efficiency is restricted to the band 247–262 Hz.

The high signal-to-noise ratio of mode 3 in a fluid-resonant configuration allows frequency tracking over an extended range of frequencies. This is illustrated in Fig. 4(c) where a 6 dB attenuation was obtained within the band 370–390 Hz. For the fluid-resonant coupling at maximum intensity (Fig. 4(d)), the accuracy of the frequency tracking is significantly enhanced by the stability of the natural mode and an attenuation of 18 to 21 dB can be obtained on the band 388–401 Hz, with a maximum efficiency at the nominal frequency of the natural mode.

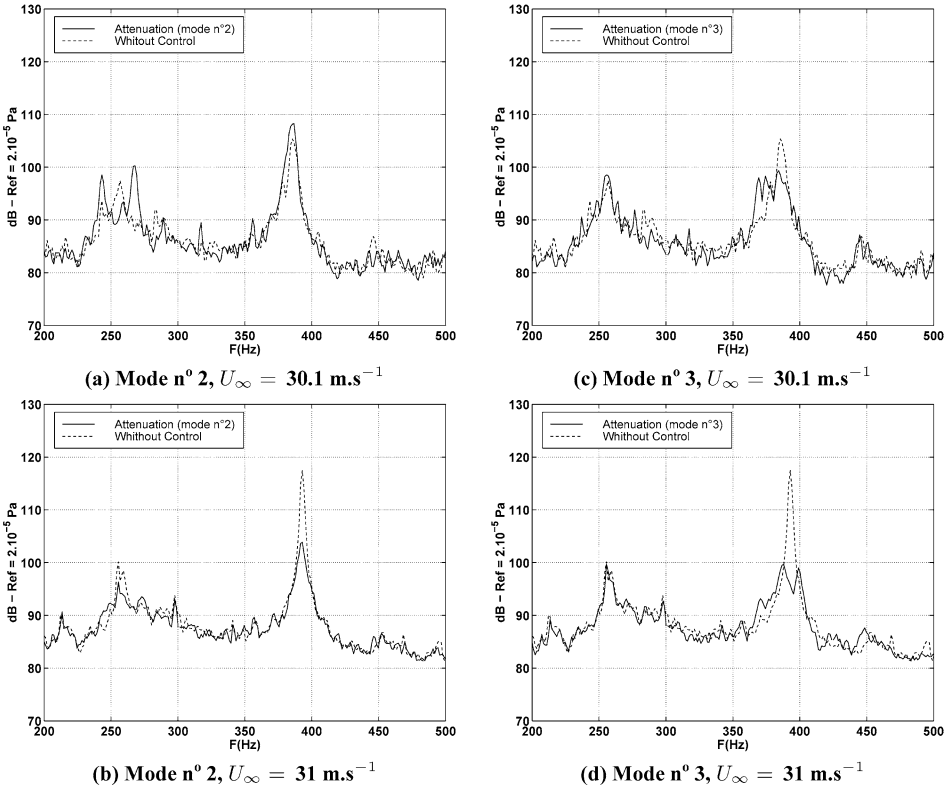

(a) Mode n^o 2, $U_\infty = 30.1$ m.s^{-1}

(c) Mode n^o 3, $U_\infty = 30.1$ m.s^{-1}

(b) Mode n^o 2, $U_\infty = 31$ m.s^{-1}

(d) Mode n^o 3, $U_\infty = 31$ m.s^{-1}

Fig. 4. Attenuation of the oscillation modes with weak or strong aeroacoustic coupling. Mode 2: (a) weak coupling; (b) decaying weak coupling. Mode 3: (c) strong coupling; (d) coupling at maximum intensity.

Fig. 4. Attenuation des modes d'oscillation en présence de couplages aéroacoustiques faibles ou intenses. Mode 2 : (a) couplage faible ; (b) couplage faible dégradé. Mode 3 : (c) couplage fort ; (d) couplage au maximum d'intensité.

These four configurations prove that such a control strategy can operate successfully on definite narrow-band modes and, to a certain extent, on modes that can fluctuate over a bounded frequency range.

3.3. Oscillations of the controlled mixing layer

The method used by Chatellier et al. [16] to identify the convective waves involved in the naturally oscillating mixing layer from phase-locked PIV measurements has been used here to characterize the efficiency of the control from an aerodynamic point of view. For each configuration, the square wave issued from the second stage of the control board (Fig. 1) was decimated to match the acquisition rate of the PIV system. Series of 100 PIV fields were acquired for 10 different phase lags covering a full period of a chosen mode of oscillations.

Fig. 5 shows results obtained for mode 3 when the aeroacoustic coupling is at maximum intensity. Results obtained in other configurations are discussed in Chatellier [17].

The post-processed experimental results clearly illustrate the modulating effect of control on the convective wave for both the attenuation and amplification cases. While Fig. 5(a) shows that the oscillations of the interface can be efficiently attenuated from $x/L = 0.6$ to 0.9, Fig. 5(c) reveals that the amplification strongly affects the shape of the oscillations and sharpens the anti-nodes of the convective wave. In both cases, the limit of the efficiently controlled area can be identified around $x/L = 0.6$, where the convective wave tends to exhibit a discontinuity. Despite the perturbing effect of control, these results agree with analytical predictions obtained by Chatellier et al. [16], and allow the identification of phase and amplitude parameters for each series of data.

Results averaged over a full period show that the amplitude parameter of the oscillations is 0.33 mm for the unforced mode, 0.43 mm during amplification and 0.28 mm during attenuation. For this mode, the corrections on the radiated sound are +5 dB in amplification and −15 to −21 dB in attenuation, while the corresponding levels of acceleration measured at the actuator are respectively 170 and 160 dB (reference: $10^{-6}\ \mathrm{m\,s^{-2}}$). In comparison, calibration tests reported in Chatellier [17] indicate that the transfer function gain between the actuator and Microphone n^o 2 is about −80 dB at 390 Hz. In consequence, if the control resulted only in local sound interferences near Microphone n^o 2, the measured sound levels indicate that the vibration level of the plate should be of the order of 200 dB for an in-phase

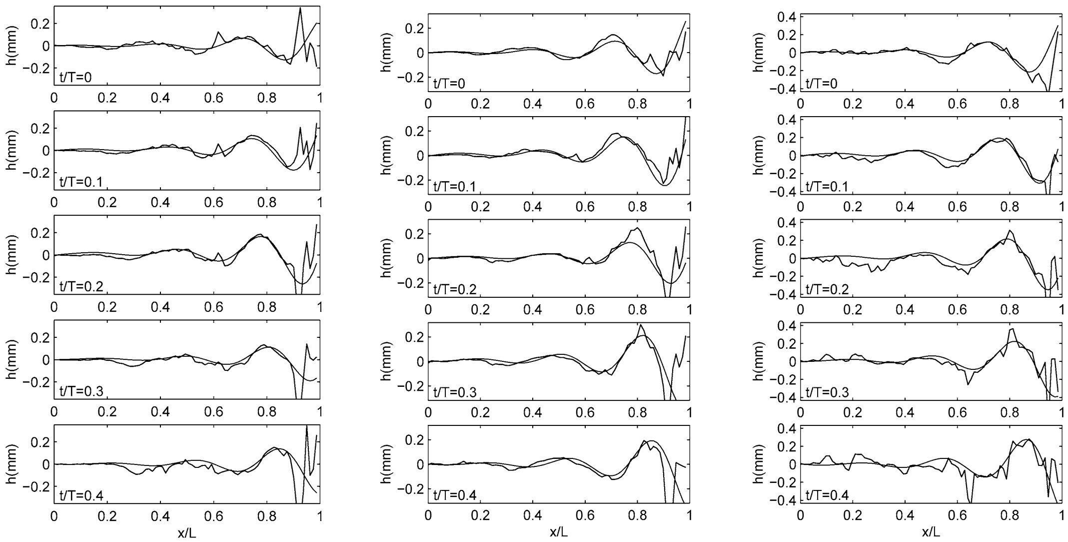

(a) (b) (c)

Fig. 5. Effect of control on the motion of the cavity interface over half a period. (a) Attenuation; (b) Natural oscillations; (c) Amplification. Bold: Experimental results; thin: analytical results with fitted amplitude and phase. $L = 150$ mm, $L/D = 1$, $W/L = 5.2$, $U_\infty = 31\ \mathrm{m\,s^{-1}}$, mode 3, aeroacoustic coupling at maximum intensity.

Fig. 5. Effet du contrôle sur les oscillations de l'interface de la cavité mesurées sur une demi période. (a) Attenuation ; (b) Oscillations libres ; (c) Amplification. En gras : résultats expérimentaux ; en traits fins : résultats analytiques ajustés en amplitude et en phase. $L = 150$ mm, $L/D = 1$, $W/L = 5{,}2$, $U_\infty = 31\ \mathrm{m\,s^{-1}}$, mode n^o 3, couplage aéroacoustique au maximum d'intensité.

amplification of the pressure signal and 195 dB if it was working as an anti-noise device. These levels are well beyond the measured values and are unrealistic in terms of mechanical vibrations, which demonstrates that the proposed device is able to modulate the radiated sound by locally controlling the flow in the vicinity of the downstream edge.

4. Conclusion

Active control of low Mach number turbulent cavity flows using a vibrating element at the trailing edge is investigated in this article. It is shown that noise radiated by the aeroacoustic modes can be modulated via an open loop circuit using a single reference microphone and a manually adjusted frequency tracking circuit.

A PIV system phase-locked with the controller is used to characterize and quantify effects of control on the oscillating mixing layer. It has been observed that control of the flow can be effectively obtained in the vicinity of the actuator, while the oscillations of the upstream part of the mixing layer appear essentially diminished. These results confirm that a local fluid-elastic coupling can be forced and used to modulate the convective wave in fluid-resonant conditions, leading to an efficient control of the radiated sound.

Further investigations should focus on the feasibility of control when no acoustic resonance is present, using hot films or hot wires as reference sensors so that the hydrodynamic features of the flow can be efficiently isolated.

Acknowledgements

This work was completed under a grant from the CNRS and the region Poitou-Charentes through the program GdR 1186: Active Fluid Mechanics.

References

[1] J.E. Rossiter, Wind tunnel experiments of the flow over rectangular cavities at subsonic and transonic speeds, Aero. Res. Counc. R. & M. 3438 (1964).
[2] H.H. Heller, D.B. Bliss, Flow-induced pressure fluctuations in cavities and concepts for their suppression, AIAA paper 75-491, 1975, pp. 281–296.
[3] L.L. Shaw, Suppression of aerodynamically induced cavity pressure oscillations, J. Acoust. Soc. Am. 66 (3) (1979) 880–884.
[4] M.J. Staneck, G. Raman, V. Kibens, J.A. Ross, J. Odedra, J.W. Peto, Suppression of cavity resonance using high frequency forcing—the characteristic signature of effective devices, in: 7th AIAA/CEAS Aeroacoustics Conference and Exhibit, Maastricht, The Netherlands, May 2001, pp. 2001–2128.
[5] M. Sunyach, J. Ffowcs Williams, Contrôle actif des oscillations dans les cavités excitées par un écoulement, C. R. Acad. Sci. 303 (12) (1986) 1085–1088.
[6] X.Y. Huang, D.S. Weaver, On the active control of shear layer oscillations across a cavity in the presence of pipeline acoustic resonance, J. Fluids Structures 5 (1991) 207–219.
[7] J. Anthoine, M. Mettenleiter, O. Repellin, J.-M. Buchlin, S. Candel, Influence of adaptive control on vortex-driven instabilities in a scaled model of solid propellant motors, J. Sound Vib. 262 (5) (May 2003) 1009–1046.
[8] V. Sarohia, Experimental investigation of oscillations in flows over shallow cavities, AIAA Journal 15 (7) (July 1977) 984–991.
[9] R.H. Cabell, M.A. Kegerise, D.E. Cox, G.P. Gibbs, Experimental feedback control of flow induced cavity tones, in: 8th AIAA/CEAS Aeroacoustics Conference and Exhibit, Breckenridge, Colorado, June 2002, pp. 2002–2497.
[10] R.L. Sarno, M.E. Franke, Suppression of flow-induced pressure oscillations in cavities, J. Aircraft 31 (1) (January 1994) 90–96.
[11] L.N. Cattafesta, III, S. Garg, M. Choudari, F. Li, Active control of flow-induced cavity resonance, AIAA paper 97-1804, 1997.
[12] C.W. Rowley, V. Juttijudata, D.R. Williams, Cavity flow control simulations and experiments, in: 43rd AIAA Aerospace Sciences Meeting, January 2005.
[13] T. Kestens, F. Nicoud, Active control of unsteady flow over a rectangular cavity, in: 4th AIAA/CEAS Aeroacoustics Conference and Exhibit, Toulouse, France, 98-2348, May 1998.
[14] T. Kestens, Etude numérique du controle adaptatif multivoies des instabilités aéroacoustiques des cavités, PhD thesis, Institut National Polytechnique de Toulouse, 1999.
[15] D. Rockwell, E. Naudascher, Review: Self-sustaining oscillations of flow past cavities, J. Fluids Eng. 100 (1978) 152–165.
[16] L. Chatellier, J. Laumonier, Y. Gervais, Theoretical and experimental investigations in low Mach number turbulent cavity flows, Experiments in Fluids 36 (5) (May 2004) 728–740.
[17] L. Chatellier, Modélisation et contrôle actif des instabilités aéroacoustiques en cavité sous écoulement affleurant, PhD thesis, Université de Poitiers, 2002.
[18] M.S. Howe, Edge, cavity and aperture tones at very low Mach numbers, J. Fluid Mech. 330 (1996) 61–84.
[19] M.S. Howe, Low Strouhal number instabilities of flow over apertures and wall cavities, J. Acoust. Soc. Am. 102 (2) (1997) 772–780.
[20] M.S. Howe, Acoustics of Fluid-Structure Interactions, Cambridge Univ. Press, Cambridge, UK, 1998.